EUROGRAPHICS '92 / A. Kilgour and L. Kjelldahl (Guest Editors), Blackwell Publishers

Volume 11, (1992), number 3

Stochastic Motion—Motion Under the Influence of Wind

Mikio Shinya*
NTT Human Interface Laboratories
3-9-11 Midori-cho, Musashino-shi
Tokyo, 180 Japan

Alain Fournier
Department of Computer Science
University of British Columbia
Vancouver, BC, V6T 1W5 Canada

Abstract

Stochastic approaches are very effective for modelling natural phenomena. This paper presents a motion model based on a stochastic process as well as physics, and proposes motion synthesis techniques for stochastic motion—motion under the influence of wind.

The motion synthesis process is modelled by a cascade system of three components: wind model, dynamic model, and deformation model. Wind models produce spatio-temporal wind velocity fields using the power spectrum and auto-correlation of wind, just like fractal geometry. Dynamic models describe the dynamic response of the systems, using equation systems or response functions. Deformation models produce deformed shapes of objects according to the geometric models of the objects and the results of the dynamic systems.

The biggest advantage of the model is its generality and consistency. The model is applicable to most of the existing trees and grass models, including structural models, particle systems, impressionist models, and 3D texture. It is demonstrated that the coupling of stochastic approaches and physically-based approaches can synthesize realistic motion of trees, grass and snow with modest computational cost.

Keywords: Computer Animation, Natural Phenomena, Stochastic Motion, Physically-based Modelling, Wind Model, Modal Analysis, Filtering, 3D Texture

1 Introduction

Modelling natural phenomena is one of the most challenging subjects in the computer graphics field, and a lot of research has already been done [1]. Stochastic models, such as fractal mountains [2,3] and particle systems [4], are important, because they show that apparently complex geometry can be produced by simple rules through a stochastic process.

As well as shape, the motion of natural objects is a fundamentally stochastic process because there are so many factors governing motion that it is almost impossible to specify them in deterministic ways. For example, the motion of a grass field and trees looks very complicated, but, at the same time, quite uniform with some stochastic characteristics, similar to fractal geometry. Thus, it should be possible to reproduce it through simple stochastic models.

Motion due to wind is an important example of stochastic motion, because wind is the dominant cause of motion in natural outdoor scenes. Wind causes ocean waves [5] and influences cloud development [6], as well as moving trees and grass.

This paper proposes a general scheme of stochastic motion, and focuses on motion models of natural objects, in particular, trees and grass, under the influence of wind. Some animation sequences have demonstrated impressive motion of grass [7], a tree [8], and leaves [9]. Those models work well in their particular situations, but over-simplification and the usage of heuristics limit their applicability. Since there are a variety of models for natural phenomena, flexibility and generality are crucial demands for motion models to assure consistency among models.

*Part of this work was done at the University of Toronto.

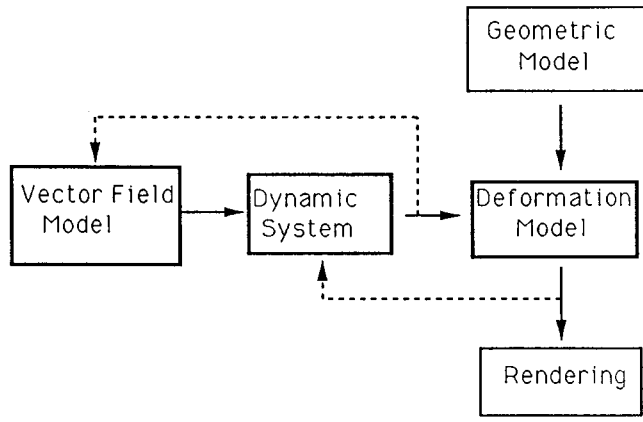

Figure 1: A stochastic motion model

First, we model the process with three components, the vector field model, the dynamic system, and the deformation model. In the context of wind, the vector field model provides wind velocity fields. The dynamic systems are spatio-temporal equation systems or response functions, which characterize motion. The deformation models convert the results of the dynamic systems into the geometrical or graphical data necessary for the rendering process. The major advantage of the scheme is that it localizes the geometric-model dependent process.

Second, the models are applied to motion due to wind, and methodologies are developed to synthesize realistic motion of trees and grass fields. Spatio-temporal characteristics of wind are introduced from the structural engineering field. Filtering techniques and modal analysis are applied to develop dynamic and deformation models.

Finally, we apply the methods to most of the existing models of trees and grass, including the structural model [10,11], the particle systems [4], the impressionist model [12], and 3D texture [13,14]. It is demonstrated that the coupling of the stochastic and physically-based approaches can synthesize natural motion of trees, grass and snow with modest computational cost. The synthesized motion shows spatio-temporal consistencies among different geometric models, which has not yet been achieved by ad-hoc methods.

2 Stochastic Motion

The process of stochastic motion is modelled by a cascade system of three components, a vector field model, dynamic system, and deformation system, as shown in Figure 1. The vector field model produces spatio-temporal vector fields, such as wind velocity fields, from specified parameters. From the given field, the dynamic system solves the dynamic equations of the objects. The result of the dynamic systems is a time sequence of dynamic variables, and, therefore, it might be a parameterized motion, not directly expressing geometrical displacement. The deformation models interpret the results of the dynamic systems and generate deformed shapes by referring to geometric models.

There should be some feedback loops in the flow. For example, when considering wind, there would be wake turbulence (feedback to the wind model from the dynamic systems), changes in drag coefficients due to changes of shape (feedback from deformation), and so on. In this paper, feedback is neglected for simplicity, but the scheme can incorporate feedback loops if necessary, although some of them might significantly increase the computation cost, for example, having to solve Navier-Stokes equations.

3 Wind Model

Wejchert et al. introduced a linearized fluid flow model to simulate the motion of leaves being blown by wind [9]. The linearized flow satisfies the Laplace equation, and thus, is mathematically identical to a static electric field. This model is appropriate for objects travelling along the flow, like leaves, but

cannot generate motion of trees and grass because the field is *temporally static*. Therefore, we absolutely need temporal variation in wind models, as well as spatial variation. Reeves at al. introduced a wind particle model for grass motion. In their model, each particle represents a small gust of wind [7], and is placed by random displacement, producing spatio-temporal variation. Unfortunately, the stochastic properties of wind were not taken into account, and careful manual adjustment is necessary to obtain satisfactory wind fields.

In this paper, we introduce a simple stochastic wind model from the structural engineering field, where the characteristics of wind are very important because structures must be designed to avoid resonating with wind. There are some models of wind velocity fields for isotropic and homogeneous conditions [15,16] that reasonably agree with actual measurements. Although these models were built for strong wind (more 10 meter/second), we found they are still good for weaker wind (about 4 meter/second), at least for graphics purposes.

3.1 Temporal Power Spectrum

The temporal characteristic of wind is low-pass in the frequency domain, where the cut-off frequency depends on the mean velocity of the field. There are three fundamental directions for wind, i.e., the mean wind direction (u-direction), the horizontal direction perpendicular to the u-direction (v-direction), and the vertical direction (w-direction). Each wind component has slightly different characteristics.

It is convenient to describe the characteristics by using the power spectrum, which is defined by

$$S_g(f) = |\int g(t)\exp(2\pi f t)dt|^2.$$

There are several experimental formulas of the power spectra of wind in uniform fields, but since there seems to be no serious difference among them for graphics purposes, we adopted a simple one that well matches observed data [15]. According to the model, the power spectra for u-, v-, w-components, S_u, S_v, and S_w, respectively, are modelled as

$$\begin{aligned} S_u &= C_0 \cdot 200(\nu/f)/(1+50\nu)^{5/3}, \\ S_v &= C_0 \cdot 15(\nu/f)/(1+9.5\nu)^{5/3}, \\ S_w &= C_0 \cdot 3.36(\nu/f)/(1+10\nu^{5/3}), \end{aligned} \tag{1}$$

where f is the temporal frequency in Hz, $\nu = fz/U(z)$, z is the height of the observation point from the ground, and $U(z)$ is the mean wind velocity at the point. The constant C_0 is the normalization constant dependent on the variance of the u-component, such that

$$\int S_u df = \text{(the variance of the u-component)}$$

The shapes of the power spectra are shown in Figure 2. The spectra have low-pass characteristics, and u-component is the dominant component of the gust.

3.2 Cross Spectrum

A cross spectrum of the wind velocity at two points, $\vec{r}_0 = (x_0, y_0, z_0)$ and $\vec{r}_1 = (x_1, y_1, z_1)$, is defined as

$$S^c(\vec{r}_0, \vec{r}_1, f) = \lim_{T\to\infty} \frac{1}{T} \int_{-T/2}^{T/2} u(\vec{r}_0, t)u(\vec{r}_1, t+\tau)dt \int_{-\infty}^{\infty} \exp(2\pi i f\tau)d\tau,$$

where u is the wind velocity. The physical meaning is the temporal Fourier transform of the spatio-temporal auto-correlation of $u(\vec{r}, t)$.

The cross spectra of u-, v-, w-components, S_u^c, S_v^c, and S_w^c are modelled by

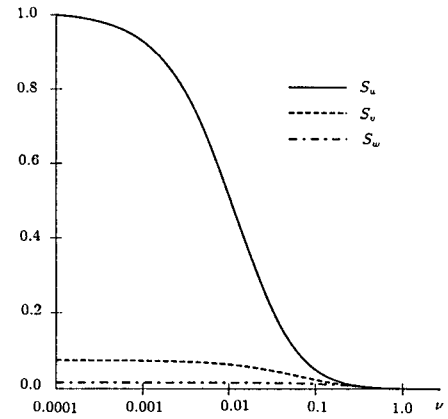

Figure 2 Power spectra of wind.

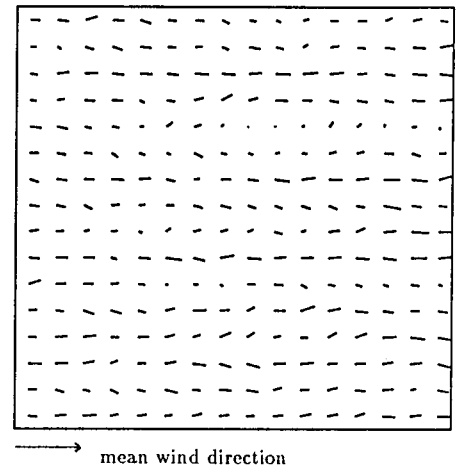

Figure 3 Wind velocity field

$$\begin{aligned} S_u^c &= \sqrt{S_u(z_0)}\sqrt{S_u(z_1)}\exp(-\xi_u), \\ S_v^c &= \sqrt{S_v(z_0)}\sqrt{S_v(z_1)}\exp(-\xi_v), \\ S_w^c &= S_w(z_0)\exp(-\xi_w), \end{aligned} \tag{2}$$

where

$$\begin{aligned} \xi_u &= f\sqrt{c_{1z}^2(z_1 - z_0)^2 + c_{1y}^2(y_1 - y_0)^2}/U(10) \\ \xi_v &= f\sqrt{c_{2z}^2(z_1 - z_0)^2 + c_{2y}^2(y_1 - y_0)^2}/U(10) \\ \xi_w &= 8f|y_1 - y_0|/U(z) \end{aligned}$$

The exponential decay coefficients, c_{1y} and c_{1z}, depend on the mean wind velocity, height (z), and surface roughness, and they range between 3 and 10. As typical values, we used $c_{1y} = 3.6$, and $c_{1z} = 6.0$. The decay coefficients for the v-component are known to be about 66% of those for the u-component, and thus, $c_{2y} = 2.4$ and $c_{2z} = 4.0$. Less study has been done on the w-component, perhaps because of its smaller energy, and we only found the cross spectrum for horizontal displacement.

3.3 Taylor's Hypothesis

Taylor's hypothesis is a widely accepted assumption that turbulence travels at the mean velocity U, expressed as

$$u(x, y, z, t) = u(x - t/U, y, z, 0), \tag{3}$$

where u is the wind velocity, t is time, and (x, y, z) is the position in the u-, v-, w-directions.

The advantage of using this hypothesis is that the dimensions of the data can be reduced from four to three.

3.4 Implementation

Since the spatio-temporal characteristics of wind are modelled by its co-spectra, FFT is very efficient to synthesize the wind velocity field. Furthermore, the periodic property of the discrete Fourier transform is convenient because modest size data can be periodically applied to a large area and/or a long animation sequence.

The procedure is outlined as follows:

1 Initialize a complex data array `Wind[f][y][z]` according to Equations 1 and 2. (For negative f, `Wind[f][y][z]= Wind[-f][y][z]`).

2 Apply FFT with y and z.

3 Multiply random phase $\exp(\phi)$ by `Wind`, where ϕ is a uniform random number from $-\pi$ to π. Keep `Wind[f][y][z]` = `wind*[-f][-y][-z]` so that the inverse transform is real. (a^* indicates the complex conjugate of a).

4 Apply inverse FFT.

5 Normalize with the specified variance.

In the current implementation, z is considered constant so that the memory space is reduced from three dimensions to two. Figure 3 demonstrates an example of the horizontal wind velocity field at a certain time in vector expression.

4 Dynamic System

4.1 Temporal Characteristics

It is well-known that motion around an equilibrium is well approximated by harmonic oscillation. More intuitively, the motion of trees and grass is oscillatory. This idea is supported by a modal analysis shown later. Since, in the real world, damping factors always exist, a damped harmonic oscillator is an appropriate model.

When a system consists of several sub-systems with different dynamic characteristics, e.g., leaves, branches and trunks of a tree, the model should become a damped coupled harmonic oscillator, or a composed RLC circuit model in the analogy of electric circuits. The equation system of a damped coupled harmonic oscillator is as follows:

$$m_i \frac{d^2 X_i}{dt^2} + \gamma_i \frac{dX_i}{dt} + \sum_j \alpha_{ij} X_j = f_i(t), \tag{4}$$

where $X_i(t)$ (i=1,2,...,n) are dynamic variables to be computed, m_i, γ_i, α_{ij} are system parameters, and f_i is applied force.

4.2 Spatial Characteristics

There are at least two ways to model spatial characteristics. One is to explicitly describe all interactions among the (sub-)systems by their equations. (In Eq. 4, α_{ij} represents interaction). This works well when sufficient information is given about geometry and mechanical properties.

However, when the properties and interactions are uniform, or not well known in detail, the spatial characteristic can be defined in a more stochastic way, using correlations or a co-spectrum.

Consider the situation where a sinusoidal force $\sin(-2\pi ft)$ is applied at $\vec{x}'$. The expected (complex) amplitude of motion at $\vec{x}$, $h(x, f)$, is assumed as

$$h(x, f) = h_t(f) h_x(\vec{x} - \vec{x}'; f), \tag{5}$$

where h_t is the (average) impedance of the system, and h_x is the spatial auto-correlation of the impedance. The auto-correlation h_x can be dependent on the temporal frequency, if necessary. For example, if the correlation decreases with frequency, we can use a function like

$$h_x = \exp(-f|\vec{x} - \vec{x}'|^2/\sigma_h).$$

4.3 Physics of motion

Physically based models generally result in very realistic motion ([17,18,19] amongst others), and it is important for the dynamic system to be based on physics as much as possible. In this section, we introduce two useful formulas: a modal analysis of uniform beams and drag force caused by wind.

Modal Analysis As demonstrated by Pentland [20], modal analysis is a powerful method for motion synthesis in computer graphics. Although it is generally difficult to analytically solve the vibration modes, there is a useful analytic solution for a simple object; a uniform beam, or uniformly mass-distributed bar. When a uniform beam is a good approximation of a trunk or branch, the results of the analysis are applicable to the dynamics of the tree motion.

For a uniform beam with length l, the mode functions and natural frequencies have been proved to be:

$$V_r(x) = B_r\{\cosh(\lambda_r x/l) - \cos(\lambda_r x/l) - \eta_r(\sinh(\lambda_r x/l) - \sin(\lambda_r x/l))\},$$

where

$$\begin{aligned} \eta &= \{\cosh(\lambda_r) - \cos(\lambda_r)\}/\{(\sinh(\lambda_r) - \sin(\lambda_r)\}, \\ \lambda_1 &= 1.875, \\ \lambda_2 &= 4.694, \\ &\cdots \\ \lambda_r &\simeq (r - 1/2)\pi, \end{aligned}$$

and

$$\omega_r^2 = \lambda_r^2\sqrt{EI/\rho A}. \tag{6}$$

The shapes of the first three modes are shown in Figure 4. For the fundamental mode $V_1(x)$, we found a useful polygonal approximation

$$(1/3)x^4 - (4/3)x^3 + 2x^2,$$

which approximates the function very well (the largest error is 1.3% of the maximum value) and satisfies the boundary conditions.

Using the function system $\{V_r(x)\}$, we can solve the damped forced oscillation problem

$$\frac{\partial^2}{\partial x^2}(EI\frac{\partial^2 v}{\partial x^2} + c\frac{\partial^3 v}{\partial x^2 \partial t}) + \rho A\frac{\partial^2 v}{\partial t^2} = p(x)f(t), \tag{7}$$

where c is a damping factor, E is Young's modulus of the beam, I is the second order moment, ρ is the (mass) density, A is the cross sectional area of the beam, and $p(x)f(t)$ is the applied force. The solution $v(x,t)$ can be expanded by the system $\{V_r\}$ as

$$v(x,t) = \sum_r V_r(x)q_t(t). \tag{8}$$

From Equations 7 and 8, the vibration of each mode is expressed by

$$\frac{d^2 q_t}{dt^2} + c\omega_r^2\frac{dq_t}{dt} + \omega_r^2 q_t = K_r f(t), \tag{9}$$

where

$$K_r = \int p(x)V_r(x)dx / \int \rho A(V_r(x))^2 dx.$$

Note that the shear force S at x is:

$$S = \frac{\partial}{\partial x}(-EI\frac{\partial^2 v}{\partial x^2}), \tag{10}$$

which can be used as a coupling force between two connected beams.

Drag Force The wind model provides wind velocity fields, but the dynamic system needs force applied to objects for its calculations. There are two major forces produced by wind. One is the force perpendicular to the wind direction, called lift, and the other is drag, parallel to the direction.

The drag F_d and lift F_l at a wind velocity U are given by

$$F_d = \frac{1}{2}\rho U^2 BC_d,\ F_l = \frac{1}{2}\rho U^2 BC_l,$$

where ρ is the density of air, C_d and C_l are the drag and lift coefficients, respectively, and B is some typical reference dimension, e.g., diameter in the case of a cylinder. Both drag and lift coefficients depend on the shape of the object and the angle between the wind and the object (the angle of attack).

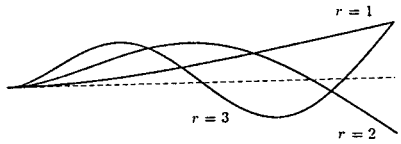

Figure 4 Vibration modes of uniform beams.

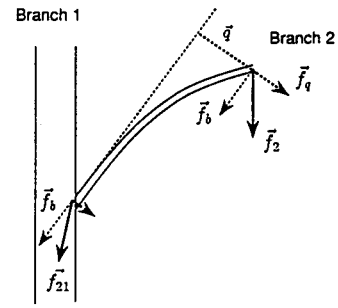

Figure 5 Coupling force between branches.

5 Deformation Model

5.1 Structural Models

Most tree models, for example, grammar-based models ([10,11]), and botanical-based models ([22]), have a tree-type structure expressed as connections among trunks, nodes, and branches, and geometrical shape data. When the dynamics of each component is well modelled by simple damped harmonic oscillation, the over-all system is a coupled damped oscillator, and the discussion in Section 4.1 can be applied. When branches and trunks can be approximated as uniform beams, the result of modal analysis discussed in Section 4.3 can be applied.

5.2 Particle System

Particle systems were introduced by W. Reeves and have produced very realistic images of forests and grass [4]. Since object shapes are defined by the trajectories of moving particles, the dynamics of defined objects are not as clear as in the structural models. However, realistic motion of grass can be created by controlling the initial condition of the particles [7].

Let $\vec{v_0} = (v_0, \theta, \phi)$ be the initial velocity vector of a particle, expressed in polar coordinates. As a result of the drag force due to the wind $\vec{f} = (f_x, f_y, f_z)$, we vibrated the initial direction, θ and ϕ, according to

$$\frac{d^2\theta}{dt^2} + \gamma_\theta \frac{d\theta}{dt} + \omega_\theta^2 \theta = f_\theta/m, \quad \frac{d^2\phi}{dt^2} + \gamma_\phi \frac{d\phi}{dt} + \omega_\phi^2 \phi = f_\phi/m,$$

where m, ω, γ are constant, and f_θ, f_ϕ are projections of the applied force onto the x-y plane, expressed by

$$f_\theta = -f_x \sin\theta + f_y \cos\theta, \quad f_\phi = f_x \cos\theta + f_y \sin\theta.$$

5.3 Impressionist Model

G. Gardner developed impressionist models and produced beautiful images of clouds and trees [12,23]. There are two elements in his method: a texture function and simple geometry (usually, quadrics). Since there is little physical relationship between the model and real trees, it is difficult to define accurate dynamic models. However, the space-invariant approach is applicable, and the physical based approach, as well, can be applied in a limited way.

Deformation of quadrics Trees in the impressionist model usually have a trunk and an envelope of leaves. Although the uniform beam model can be applied to the trunk, it is not applicable to the envelope because the structure of the branches is unknown. Thus, we have to assume a structure to obtain deformation. For convenience, we take the simple assumption that all branches are horizontal and the trunk is vertical. Next, we neglect the vibration of branches because it can be modelled through the deformation of texture. This simplifies deformation into just a horizontal shift. The displacement of the envelope is equal to that of the trunk at the same height. This also simplifies rendering because the deformation can be done on the screen space as displacement mapping [24].

Texture Since texture itself has no structure, the space-invariant filtering technique, discussed in Section 4.2, is applied. A proper spatio-temporal response function is assumed, and then multiplied by the wind velocity field (or drag force field) in the Fourier domain. By inverse FFT, a vibration field $\vec{d}(x,y,t) = \vec{d}_0(y, t - x/U)$ is obtained. To make the visual motion smooth, the vibration is projected onto the tangent plane of the envelope.

5.4 3D Texture

Kajiya [13] and Perlin [14] successfully applied 3D texture to furry objects. Although there are still unsolved problems (e.g., texture synthesis, anti-aliasing, and mapping function), we believe it is a potentially powerful model for natural objects, including grass and trees.

Since 3D texture is difficult to directly obtain from measurements, unlike 2D texture, it is most likely to be created from some shape models through 3D scan-conversion. In this case, if dynamics and deformation can be defined in the shape model, motion of 3D texture is easily introduced by solving the dynamics and deformation of the model, and then producing the corresponding deformed 3D texture.

6 Experiments

6.1 Structural Models

The uniform beam model was applied to bamboo modelled by simple rules similar to Aono's model. Trunks are cylindrical tubes, branches are cylinders, and leaves are polygons. The relevant second moment of cross-sectional area of a thin tube, I_t, and that of a cylinder, I_b, are:

$$I_t \simeq \pi r^3 \delta,\ I_b = \pi r^4,$$

where r is the radius and δ is the tube width.

constants The constants involved in Eq. 7 (ρ, E and c) are determined in the following way. First, the mass density ρ is set as $\rho = 0.8$ gram/cm^3 by measurement. Next, Young's ratio E and the viscous coefficient c are determined according to the natural frequency and the damping time. From Eqs. 6 and 7,

$$E = (2\pi f)^2 (1/13.0) l^4 \rho r^{-2},\ c = 2/(\tau_0 (2\pi f)^2),$$

where f is the fundamental natural frequency in Hz, τ_0 is the damping time in seconds, and r and l are the radius and the length of the branch being considered. Currently, we use $f = 2$ Hz, $\tau_0 = 1$ sec for a branch of $l = 1$ m, $r = 0.005$ m, resulting in $E = 3.89 \times 10^8$ and $c = 3.0 \times 10^{-4}$.

Since leaves are flat polygons, the drag coefficient is set at 2.0 kg/m^3 according to [15].

Coupling force P. Isaacs and M. Cohen modelled tree dynamics with spring-linked rigid branches[19], assuming no deformation of branches but changes in angles between connecting branches. In reality, however, there is little change in the angles between branches but large deformation of branches. Thus, we took another approach: *rigid connections between deformable branches.*

Consider the situation shown in Figure 5, where force $\vec{f}_2$ is applied to Branch 2. The applied force perpendicular to the branch, $\vec{f}_q$, causes deformation $\vec{q}$ of Branch 2, which applies shear force to Branch 1. On the other hand, the parallel component $\vec{f}_b$ 'transmits' through Branch 2 (since deformation along the branch direction is negligible), and is applied to Branch 1. Using Eq. 10, the coupling force from Branch 2 to Branch 1, $\vec{f}_{21}$, becomes:

$$\vec{f}_{21} = \vec{f}_b + EIV'''(0)\vec{q}.$$

Figure 6 Combination of different models.

Results Plate 1* shows a frame from a sequence of bamboo swaying. The wind model and dynamic simulation create very realistic motion. The bamboo consists of a trunk and 2942 branches, and the dynamic system calculations took 0.64 CPU seconds per frame on a Personal IRIS 4D/25. Plate 2* also shows a frame of bamboo in a particle grass field.

The dynamic system considered only the fundamental mode and neglected the rest because the power of the second mode is small (1% for the trunk in this example). However, higher order mode analysis can be implemented simply by solving mode equations independently and summing up the resulting deformations.

6.2 Combination of different models

One of the advantages of the proposed approach is that the motion of different types of object can be calculated in a unified way. This feature makes it easy to use different kinds of models in a scene and maintain consistency among them.

The scene shown in Figure 6 consists of a structural model (bamboo), an impressionist model (grass field), a 3D texture (rice field), and a particle system (snow). The motion looks very realistic with harmony among all models. Futhermore, there is no need to tune parameters; we just used the same wind velocity field.

7 Conclusion

We have introduced a new class of stochastic motion—motion under the influence of wind. The model for the motion consists of three components: a wind model, dynamic model, and deformation model. The stochastic property of wind in uniform environments is introduced from the structural design field.

System dynamics were modelled by damped harmonic oscillator models, and spatial interactions were described by equation systems or average response functions. Deformation models were developed for structured-tree models, particle systems, impressionist models, and 3D texture based system. In particular, modal analysis of uniform beams was introduced for tree deformation.

The coupled stochastic approach and the physically-based approaches were successfully achieved in most of the existing models of trees and grass, including structural tree models, particle systems, impressionist models, and 3D texture. The experiments demonstrated realistic motion with consistencies in time and space and between models. The simple object dynamics and wind model keep

* See page C–469 for Plates 1 and 2.

the computational cost at a reasonable level with little sacrifice in visual realism. There is always a trade-off between quality and cost, and we believe that our compromise is reasonable, considering the final realism and current computing power.

References

[1] A. Fournier, 'The Modelling of Natural Phenomena,' Graphics Interface '89, pp. 191-202, 1989.

[2] B. Mandelbrot, 'The Fractal Geometry of Nature,' W. H. Freeman and Co., 1982.

[3] A. Fournier, D. Fussell, L. Carpenter, 'Computer Rendering of Stochastic Models,' Comm. of ACM **25** (6), pp. 371-384, 1982.

[4] W. T. Reeves, 'Particle Systems–A Technique for Modelling a Class of Fuzzy Objects,' Computer Graphics **17** (3), pp. 359-376, 1983.

[5] A. Fournier, W. T. Reeves, 'A Simple Model of Ocean Waves,' Computer Graphics **20** (4), pp. 164-172, 1986.

[6] J. T. Kajiya, B. P. Von Herzen, 'Ray Tracing Volume Densities,' Computer Graphics **18** (3), pp. 165-174, 1984.

[7] W. Reeves and R. Blau, 'Approximate and Probablistic Algorithms for Shading and Rendering Structured Particle Systems,' Computer Graphics **19** (3), pp. 313-322, 1985.

[8] Nelson Max, SIGGRAPH'87 Film and Video Show, 1987.

[9] J. Wejchert and D. Haumann, 'Animation Aerodynamics,' Computer Graphics **25** (4), pp. 19-22, 1991.

[10] M. Aono, T. L. Kunii, 'Botanical Tree Image Generation,' IEEE CG&A **4** (5), pp. 10-34, 1984.

[11] A. R. Smith, 'Plants, Fractals, and Formal Languages,' Computer Graphics **18** (3), pp. 1-10, 1984.

[12] G. Y. Gardner, 'Simulation of Natural Scenes Using Textured Quadric Surfaces', Computer Graphics **18** (3), pp. 11-20, 1984.

[13] J. T. Kajiya, T. L. Kay, 'Rendering Fur with Three Dimensional Textures,' Computer Graphics **23** (3), pp. 271-280, 1989.

[14] K. Perlin, E. M. Hoffert, 'Hypertexture', Computer Graphics **23** (3), pp. 253-262, 1989.

[15] E. Simiu, R. H. Scanlan, 'Wind Effects on Structures: An Introduction to Wind Engineering', John Wiley & Sons, 1978.

[16] J. Maeda, M. Makino, 'Power Spectra of Longitudal and Lateral Wind Speed near the Ground in Strong Winds,' Journal of Wind Engineering and Industrial Aerodynamics **28**, pp. 31-40, 1988.

[17] D. Terzopoulos, J. Platt, A. Barr, 'Elastically Deformable Models,' Computer Graphics **21** (4), pp. 205-214, 1987.

[18] J. K. Hahn, 'Realistic Animation of Rigid Bodies,' Computer Graphics **22** (4), pp. 299-306, 1988.

[19] P. M. Isaacs, M. F. Cohen, 'Controlling Dynamic Simulation with Kinematic Constraints, Behavior Functions and Inverse Dynamics,' Computer Graphics **21** (4), pp. 215-224, 1987.

[20] A. Pentland, J. Williams, 'Good Vibrations: Modal Dynamics for Graphics and Animation', Computer Graphics **23** (3), pp. 215-222, 1989.

[21] M. Paz, 'Structural Dynamics -Theory and Computation,' Van Nostrand Reinhold Company, 1985.

[22] P. de Reffye, C. Edelin, J. Francon, M. Jeager, C. Puech, 'Plant Models Faithful to Botanical Structure and Development,' Computer Graphics **22** (4), pp. 151-158, 1988.

[23] G. Y. Gardner, 'Visual Simulation of Clouds,' Computer Graphics **19** (3), pp. 297-303, 1985.

[24] R. L. Cook, 'Shade Tree,' Computer Graphics **18** (3), pp. 223-231, 1984.